

# AO12: To m-infinity and beyond...

Candidate number: 51265

Supervisor: Dr D. Peters

Word count: 5700

## Abstract

In this project I designed and built a goniometer, which is needed to determine the refractive index of some mineral aerosols, including Saharan dust and volcanic ash. I tested the instrument by investigating the refractive index of the sample holder (a semicircular glass block with a refractive index of 1.5) by measuring the reflectance at different angles of incidence. The glass sample holder was not of high enough purity glass, nor was the curved surface manufactured to a good enough quality, to find the refractive index of an aerosol. However, investigations indicate that if a sample holder of high enough purity and quality could be sourced, making the limiting factor on the data the instability of the laser; the instrument could be used to find the refractive index of an aerosol to within a standard deviation of 0.06.

## 1 Introduction

Atmospheric aerosols<sup>1</sup> play important roles in the stability of our climate. Their effect is both direct, by affecting the transfer of radiation through scattering direct sunlight and scattering and absorbing infra-red radiation [1] [2] [3]; and indirect, by changing cloud properties, acting as cloud condensation nuclei and affecting cloud lifetime [3]. Aerosols can also affect atmospheric chemistry, as they may act as catalysts or as a reservoir for reactive gases [2].

Mineral dust is present in the atmosphere in a large range of sizes, and so has a considerable impact upon the absorption of infra-red radiation at many wavelengths [4]. According to [5], the Sahara desert is a particularly significant source of mineral dust in the atmosphere. Large quantities of

<sup>1</sup>solid or liquid particles suspended in the air

sand are eroded off the North West of Africa and transported westward across the Atlantic Ocean, creating a layer of aerosol in the atmosphere. Eruptions from volcanoes are another significant source of mineral dust in the atmosphere [2].

It is important to have a good knowledge of the optical properties of each aerosol, so that corrections can be made to account for the aerosol's contribution to the signal in a remote sounding retrieval. In addition, it allows the use of remote sounding to investigate the amount and distribution of the aerosol. Finally, a good knowledge of an aerosol's optical properties is important in order to estimate its radiative forcing<sup>2</sup>. The radiative forcing by aerosols remains one of the largest uncertainties in climate simulation [3], mainly due to lack of knowledge about aerosol optical properties.

Optical properties are determined by the refractive index,  $m$ , of the material. The refractive index of a medium is defined as

$$m = \frac{v}{c} = \frac{\omega}{kc} = \sqrt{\epsilon_r} = n + i\kappa, \quad (1)$$

where  $v$  is the speed of light in the medium,  $c$  is the speed of light in a vacuum, and  $\epsilon_r$  is the relative permittivity of the medium. The amount of light absorbed by a material is determined by the imaginary part of the refractive index,  $\kappa$ ,

$$I = I_0 e^{(-\alpha x)}, \quad (2)$$

where  $I$  is intensity,  $\alpha = \frac{2\omega\kappa}{c}$  and  $x$  is the distance travelled by the radiation within the medium. The amount of light reflected by the surface of an absorbing medium is determined by both the real and imaginary parts of the refractive index, for more detail see the Fresnel equations for absorbing materials given in section B in the appendix. The

<sup>2</sup>a measure of the influence a factor has in altering the balance of incoming and outgoing energy in the Earth-Atmosphere system [3]

refractive index is often dependent upon the wavelength of the incident radiation, especially if it is near an absorption band of the material [6].

A team in the Earth Observation Data Group of Oxford University Atmospheric Physics Department has been using a method described in [6] to determine the refractive index of Saharan dust and volcanic ash at infrared wavelengths. They suspend the aerosol in air, and then use a measurement of the transmission of infrared radiation through the cell containing the aerosol to determine the amount of scattering and absorption by the aerosol. This is then related to the refractive index, using Mie scattering theory and a lognormal size distribution for the number of particles with radius between  $r$  and  $r + dr$ . To fit the refractive index to the measurements of the extinction using a Levenberg-Marquardt least squares fit, they use a damped harmonic oscillator model to represent the molar polarisability, which may be related to the complex dielectric constant,  $\epsilon_r$ , via the Lorentz-Lorentz relation. This gives

$$\epsilon'(\nu) = \epsilon_\infty + \sum_{j=1}^p \frac{S_j(\nu_j^2 - \nu^2)}{(\nu_j^2 - \nu^2)^2 + \gamma_j^2 \nu^2} \quad (3)$$

$$\epsilon''(\nu) = \sum_{j=1}^p \frac{S_j \gamma_j \nu}{(\nu_j^2 - \nu^2)^2 + \gamma_j^2 \nu^2} \quad (4)$$

where  $\nu$  = wavenumber,  $j$  = band number,  $p$  = total number of bands in infra-red wavelengths,  $\gamma$  = band width,  $S$  = band strength,  $\epsilon_r = \epsilon' + i\epsilon''$  and  $\epsilon_\infty$  is a fixed parameter which may be determined from measurements of  $\epsilon_r$  at optical wavelengths. *The aim of this project is to help determine this  $\epsilon_\infty = m_\infty^2$  of Saharan dust and volcanic ash at 635nm for use in the model.*

A previous study on Saharan dust [1], at 550nm indicated that  $n$  is within the range 1.51 to 1.56 and  $\kappa$  is within the range 0.0001 to 0.0046. A previous study on volcanic ash [7] indicates that  $n$  is within the range 1.52 to 1.53, and  $\kappa$  is within the range  $1.0 \times 10^{-3}$  to  $1.5 \times 10^{-3}$ .

I am using the first person in this report to emphasise where the work was all my effort.

## 2 Theory

### 2.1 The Fresnel Equations

The propagation of electromagnetic waves is governed by Maxwell's equations. In an insulating non-magnetic medium they reduce to

$$\begin{aligned} \nabla \cdot \mathbf{E} &= 0 & \nabla \cdot \mathbf{H} &= 0 \\ \nabla \times \mathbf{E} &= -\mu_0 \frac{\partial \mathbf{H}}{\partial t} & \nabla \times \mathbf{H} &= \epsilon_r \epsilon_0 \frac{\partial \mathbf{E}}{\partial t} \end{aligned} \quad (5)$$

where  $\epsilon_0$  and  $\mu_0$  are the permittivity and permeability of free space,  $\epsilon_r$  is the complex dielectric constant,  $\mathbf{E}$  and  $\mathbf{H}$  are the electric and magnetic fields, and  $|\mathbf{E}| = \frac{\mu_0 c}{\sqrt{\epsilon_r}} |\mathbf{H}|$ .  $\mathbf{E}$  and  $\mathbf{H}$  are both perpendicular to each other and to the direction of propagation, and are of the form  $\mathbf{X} = \mathbf{X}_0 e^{i(\mathbf{k} \cdot \mathbf{r} - \omega t)}$ .

Across a boundary between media of different dielectric constants, the components of  $\mathbf{E}$  and  $\mathbf{H}$  that are parallel to the surface are constant. To satisfy these boundary conditions, an incident wave must be partly transmitted and partly reflected.

Applying the boundary conditions to the case where electric field is polarised in the plane of incidence you get

$$\begin{aligned} &E_{i0} e^{i(k_i x \sin \theta_i + k_i z \cos \theta_i - \omega_i t)} \cos \theta_i \\ &- E_{r0} e^{i(k_r x \sin \theta_r + k_r z \cos \theta_r - \omega_r t)} \cos \theta_r \\ &= E_{t0} e^{i(k_t x \sin \theta_t + k_t z \cos \theta_t - \omega_t t)} \cos \theta_t. \end{aligned} \quad (6)$$

where  $i$  indicates incident radiation,  $r$  indicated reflected,  $t$  is the transmitted, and  $\theta$  is the angle between the direction of propagation and the normal to the surface in the plane of incidence. As this statement is true for all  $t$  and  $x$ , we see that the frequency must remain constant, so  $km$ , (see equation (1)) must also be constant. Therefore, the reflection is specular ( $\theta_i = \theta_r$ ) and Snell's law of refraction may be derived

$$\sin \theta_i = m \sin \theta_t \quad (7)$$

where  $m = m_2/m_1$ ,  $m_1$  is the refractive index of the first medium, and  $m_2$  the refractive index of the second.

The boundary condition for the magnetic field gives

$$\begin{aligned} &H_i + H_r = H_t \\ \text{so } &E_i + E_r = m E_t. \end{aligned} \quad (8)$$

Equations (6) and (8) may be combined to give the Fresnel equation for the reflectance of light which is polarised in the plane of incidence. When the material is non absorbing (glass or air, for example),  $m = n$  and the amplitude ratio of the electric fields is real and the parallel reflectance may be derived to be (9). See the fit on the data in figure 6 in section 4.2.1 for a plot of parallel reflectance vs incident angle.

$$R_{\parallel} = \left| \frac{E_{r0}}{E_{i0}} \right|^2 = \left[ \frac{n^2 \cos \theta_i - \sqrt{n^2 - \sin^2 \theta_i}}{n^2 \cos \theta_i + \sqrt{n^2 - \sin^2 \theta_i}} \right]^2. \quad (9)$$

The same boundary conditions may also be applied to the problem in which the electric field is polarised in the plane perpendicular to the plane of incidence, giving Fresnel's equation for the perpendicular reflectance (10). See the fit on the data in figure 5 in section 4.2.1 for a plot of perpendicular reflectance against incident angle.

$$R_{\perp} = \left| \frac{E_{r0}}{E_{i0}} \right|^2 = \left[ \frac{\cos \theta_i - \sqrt{n^2 - \sin^2 \theta_i}}{\cos \theta_i + \sqrt{n^2 - \sin^2 \theta_i}} \right]^2. \quad (10)$$

When the material absorbs some of the incident radiation the ratio of electric fields is complex and so the algebra is more complicated, but the Fresnel equations may still be derived and are included in section B in the appendix.

At normal incidence the complex Fresnel equations both reduce to

$$R = \frac{(n-1)^2 + \kappa^2}{(n+1)^2 + \kappa^2}. \quad (11)$$

## 2.2 The Aerosol Solution

The Fresnel equations are only applicable when the radiation is incident upon a flat surface<sup>3</sup>. This may be achieved by suspending the aerosol in water, as in [8]. When a solid powder is mixed with a liquid, [8] finds that if the size parameter  $x$  ( $= \frac{2\pi a}{\lambda}$  where  $a$  = powder particle radius) is less than one, you can use the equivalent mixture approximation for the refractive index,

$$m = m_1 f_1 + m_2 f_2, \quad (12)$$

<sup>3</sup>or at least flat to  $\lambda/10$  [10]

where  $m_i$  is the refractive index and  $f_i$  is the volume mixing ratio of medium  $i$ . However, if  $x > 1$ , [8] shows that the effective medium approximation gives large errors and you must use their more complicated model, given in [8], to determine the refractive index of the solid.

## 2.3 Methods of determining refractive index

### 2.3.1 The Critical Angle

If the second medium has a lower refractive index than the first, then using Snell's law, (7), you can see that at angles of incidence greater than some critical angle there becomes no real solution for the angle of transmittance. The light undergoes total internal reflection, see the fit on the data in figure 7 in section 4.2.2. The smallest angle at which this phenomenon is observed is known as the critical angle, given by

$$\sin \theta_c = n. \quad (13)$$

The critical angle may be determined from experimental data by finding the angle at which there is a maximum in  $\frac{\partial R}{\partial \theta_i}$ . This method was used to determine the real part of the refractive index of a biological photochrome in [9].

### 2.3.2 Brewster's angle

At Brewster's angle, light which is polarised in the plane of incidence is not reflected by the medium's surface, see figure 6 in section 4.2.1. This angle of incidence is given by

$$\tan \theta_B = n \quad (14)$$

the derivation of which may be found in [10].

When the refractive index has a non-zero imaginary component, the parallel reflectance does not go to zero. However, it does reach a local minimum as before, so may still be used as a measure of refractive index. At Brewster's angle, unlike at the critical angle, there is no sharp change in reflectance with incident angle, and so an exact measurement of Brewster's angle is more difficult.

### 2.3.3 Fitting a model to the reflectance - angle data

The Fresnel equations (9) and (10) (or their equivalents for an absorbing material) may be used to

model the reflectance at each angle of incidence. The model may then be fitted to observed data by varying the refractive index, using a Levenberg-Marquardt least squares fit, as in [8]. This method has the advantage of using all of the available data from measurements of reflectance at each angle of incidence.

### 2.3.4 Transmission at normal incidence

The imaginary component of the refractive index of a material may be determined from the transmission at normal incidence, using equation (2), if the sample thickness is known. Care must be taken to account for reflections from the bottom and top of the material, using equation (11).

### 2.3.5 Refractive index matching

A Becke line is a band or rim of light that is visible along a crystal boundary in plane-polarised light. If the crystal is surrounded by a liquid of the same refractive index, this line disappears. However, the only liquids with refractive indices close to that of the aerosol<sup>4</sup> are toxic oils, and this method is only applicable to optically resolvable particles, so I will not be using this method in this case.

## 3 The Experiment

### 3.1 The Specification

In order to use the methods described above, you need to be able to measure the magnitude of the specular reflection of plane polarised light from many different angles of incidence. To do this I designed and built a goniometer which rotates a laser and detector around the sample.

The critical angle technique needs a good angular resolution. The laser creates a finite sized spot on the sample so the detector needs to be far enough away so that the angle subtended by the laser spot at the detector is less than half the angle between positions, as so to achieve the maximum resolution possible.

---

<sup>4</sup> $\approx 1.53$  [1]

### 3.2 The Design

Stepper motors control the movement of a laser diode and silicon photodiode detector around the sample. The angular resolution is improved by using the stepper motor to move a small pulley which drives a larger pulley that moves the laser or detector arm. The stepper motors are powered and controlled by a microcontroller. All the hardware and electronics are contained within a black light-tight box, so that the laser can be used safely and without interference from background light in the lab. I made the box from anodised aluminium optical rails, the sides, roof and door from black hardboard, and the bottom from an anodised aluminium breadboard.

#### 3.2.1 Laser and detector

The laser and detector were attached to aluminium rods, whose movement was controlled by the stepper motors. The microcontroller ADC (analogue to digital converter) can take a maximum current of 0.6 Amps [11] so I kept the weight of the laser, detector and mounting equipment to a minimum when choosing the parts to order. I then calculated the torque that they would exert upon the stepper motors, and purchased stepper motors that would draw an appropriate current.

The laser was stopped down with an iris to improve the angular resolution. However, there was a lot of diffraction from the edge of the iris, so in future it would be wise to put a second iris in front of the first, to block this diffraction. The laser power was stable to within 1.6%, found by monitoring laser power over 1 hr 30 mins, a graph of the results is shown in section C in the appendix.

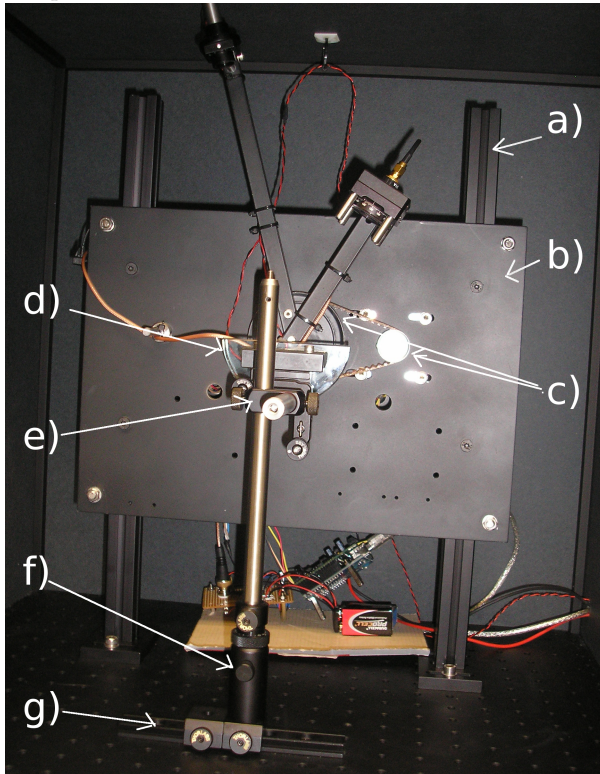
To make the alignment process easier, I chose a detector with a detecting area of 4 mm<sup>2</sup>. When the detector was in place in the equipment, the finite area and response function meant that the detector had a tolerance of  $\pm 0.6^\circ$  (see section G in the appendix) for laser misalignment. In front of the detector I mounted a linear polariser inside a graduated rotator, so that it was possible to rotate the polariser through 90°.

#### 3.2.2 Movement

See figure 1 and figure 2 for photographs of the equipment. I drew many technical drawings in or-

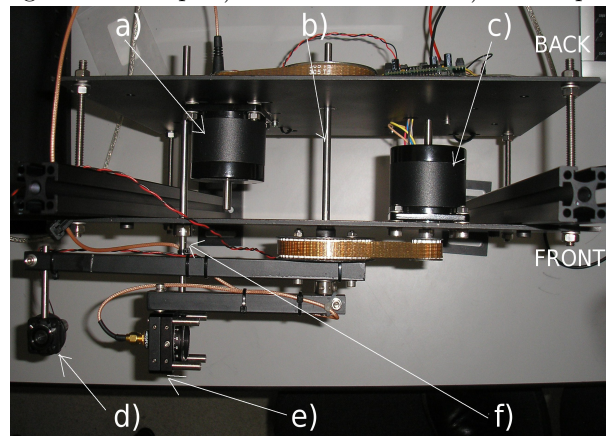
der to purchase parts of the right size, and to get the rods and aluminium sheets machined to my specifications.

Figure 1: A photograph of the equipment from the front. a) Vertical optical rails. b) Aluminium sheet, to which the stepper motors, optical rails, and electronics are attached. Sprayed black to avoid extra reflections of laser light. c) Two pulleys connected by a belt which control the movement of the laser rod. d) The glass sample holder. e) The kinematic prism mount, with screws to finely adjust the inclination of the sample. f) Translating post holder, allowing fine height adjustment of the sample. g) Dovetail rail allowing side to side adjustment of the sample.



The front faces of the pulleys were not perpendicular to the axle hole through the middle of them, so in order to get the laser aligned with the detector, the laser rod needed to be secured at an angle to the front face of the pulley. To do this I put two crinkly washers on each of the two screws holding the laser rod in place, and then tightened the screws

Figure 2: A photograph of the equipment from the top. a) The stepper motor controlling the detector. The motor rotates the pulley on the back of the equipment. This pulley rotates the axle. The rod holding the detector is clamped on to the axle at the front of the equipment. b) Axle. c) The stepper motor which controls the laser. The motor rotated the pulley on the front of the equipment. A flanged bearing allows the pulley to freely rotate around the axle. The rod holding the laser is screwed on to the front of this pulley. d) Laser at home position against the stop. e) Detector at home. f) The stop.



by different amounts.

### 3.2.3 The Sample

See figure 1 for a photograph of the sample mounting system.

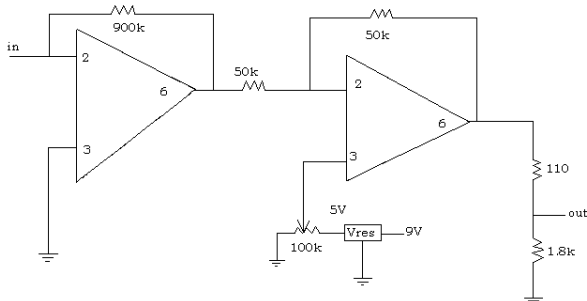
The prism mount could be used with a clamp to secure a glass slide, or could be screwed in to the back of a semicircular glass block as in the photograph in figure 1 and drawing in figure 4 in section 4.2, allowing the equipment to be used with many methods.

### 3.2.4 The Electronics

The signal from the detector has to be amplified before being passed to the ADC. I built the amplifying circuit using two operational amplifiers, see figure 3 for a circuit diagram.

The first amplifier amplifies (and reverses the sign of) the detector signal. An inverting oper-

Figure 3: Circuit diagram of the electronics.



ational amplifier works by setting the same voltage to pin 2 (signal in) as pin 3 (grounded) - i.e. grounding pin 2. All current must then run through the external resistor that connects the pin 2 to pin 6 (the output pin). The voltage at pin 6 is thus  $-I_{in}R_{ext}$ , so the value of the external resistor determines the gain of the amplifier. I added a second inverting amplifier of unity gain in order to reverse the sign of the signal again, as the microcontroller cannot read in negative voltages. I set the gain set such that when the dark current<sup>5</sup> was just above zero, the maximum laser signal was just below the threshold of the ADC (5.5 V [11]). All amplifiers have a small offset voltage between pin 2 and pin 3. If the signal coming in creates a voltage that is smaller than this offset, the output voltage may be of the wrong sign. As the ADC can not read in negative voltages, at first it was giving out a value of zero at small signals. In order to rectify this problem, I applied a voltage bias to the second amplifier, which added an offset voltage to the signal. The magnitude of the offset was controlled by a potential divider, and set so that all voltages entering the microcontroller were positive. This solved the problem but this, combined with the large gain, made the output of the circuit very temperature sensitive. I attempted to stabilise the temperature by shutting the blinds and turning on the air conditioning in the laboratory, but the equipment did heat up throughout the day (possibly due to the heat given off by the power pack and laptop) so

<sup>5</sup>the current from the detector when there is zero incident light

the signal drifted and I had to take regular measurements of laser power and dark current. After the amplifiers, the signal was passed through a potential divider to make sure that no more than the threshold voltage would be passed to the ADC. See section D in the appendix for a photograph of the circuit.

The microcontroller consists of a preassembled Arduino board and a motor shield kit, which I had to build, see section D in the appendix for a photograph of the microcontroller.

### 3.3 Software

The microcontroller is controlled by sketches written in C which are uploaded to the board via a serial port on the computer. I used two sketches during the experiment; transcripts are included in section H in the appendix

I wrote the first sketch to take a reading of the detector signal every 200 ms, and print each reading back to the screen of my laptop via the serial port, ready to be saved as a .txt file. I used this sketch to take a measurement of the dark current or laser power.

The second sketch is the main sketch with which I controlled my motors and took detector readings. Commands were passed to the board via the serial port. You could move the arms to a position (used when aligning the equipment), or scan over many angles of incidence (used to take the data).

### 3.4 Analysis

Running a scan on the sample gave me a .txt file containing 10 readings at each position of the stepper motor (every  $0.29^\circ$ ) between two angles of incidence. I wrote programs in IDL to read in the file and interpret the data, using equation (15), to give the reflectance vs incident angle data.

$$\text{Reflectance} = \frac{\text{mean of the 10 readings} - \text{dark}}{\text{total} - \text{dark}}$$

$$\text{Incident angle} = \left| \frac{\text{position} - \text{normal}}{\text{no. steps/degree}} \right| \quad (15)$$

The refractive index could be found by running a function which performs a Levenberg-Marquardt

least squares fit on the data, by running my IDL program to find the critical angle or by plotting the data to find Brewster's angle or the critical angle by eye (where applicable). To perform the Levenberg-Marquardt least squares fit I chose to use a function called MPFITFUN [12]. You pass the function an array of data and errors, a model to fit the data to, and a start value for the parameter that it is fitting. I ran some tests and found that the start value must be within 140% of the actual parameter value so that it converges to the correct local minimum.

## 4 Results

### 4.1 The refractive index of the glass

To test the equipment I first tried it on the semi-circular glass sample holder. I used a Bruker IFS 66V/s infrared spectrometer to give a separate measurement of the refractive index. The spectrometer takes a measurement of the specular reflectance at many wavelengths and performs a Kramer's Kronig transformation on the spectrum (for more information see [10]). The interpreting program gave  $n \approx 1.5$  but did not supply an error.

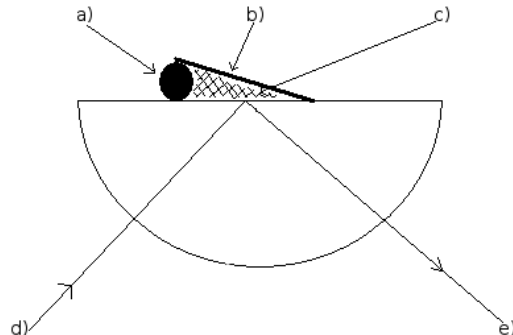
### 4.2 The First Method

See figure 4 for a ray diagram describing the first method. By taking the data from the bottom of the semicircle, the reflected signal should be from the glass-sample interface, so it should be possible to use the critical angle method to find the refractive index. Also, it is easy to eliminate the signal from the second surface and make analysis easier, by putting the sample-air surface at an angle, as in figure 4. Using a semicircular sample holder instead of a prism, as in [9], means that data analysis and detector positioning is simpler as the beam is not bent as it enters the glass.

#### 4.2.1 Measurements from the top

Before taking a scan, I had to align the laser, detector and sample, so that the specular reflection was always incident upon the detector. This was difficult as there were so many degrees of freedom, and many of the alignment processes interacted. This was made slightly easier due to the relatively large area of the detector. Detailed instructions on how

Figure 4: First method design. a) O ring. b) Glass slide at angle. c) Aerosol-water mixture. d) Laser. e) Detector.



to align the apparatus are included in section E in the appendix.

To use MPFITFUN to fit the data I first had to create an array of errors. The main sources of error were instability of the laser, the fact that you could only find normal to within half a step, lost steps by the stepper motor, and diffuse reflectance from bumps on the sample surface. To evaluate the effect of each of these errors on the fitted refractive index I used Monte Carlo simulations. For each error, I simulated 1000 measurements with a random noise at a magnitude and angular dependence similar to that of each error and used the fitting function on each simulation to estimate the refractive index. I then found the standard deviation of the refractive indices found. The results of these simulations are presented in table 1. It is clear that laser instability is the largest error.

I was then in a position to find the refractive index of the glass. I took 5 scans of the glass block at each polarisation, from normal to  $85^\circ$  angle of incidence. I ran the fitting function on both polarisations (passing it an error from the standard deviation of the 10 readings at each position, and error from the possibility that the normal in the calculations was half a step from the actual normal and a skewed error to account for diffuse reflectance from surface roughness at high angles), and found the Brewster angle of the parallel polarisation. Results are presented in table 2, and see figure 5 and figure 6 for graphs of perpendicular and parallel polarisations, respectively.

Table 1: Errors on measurement of the reflectance from the top

Error source	Description	standard deviation of fitted n
Laser instability	Laser power constant to 1.6% found from 1hr 30 min monitoring	0.040
Half a step out	Can only get to normal to within half a step	< 0.00001
Lost step	Laser lost 1 step in 2000, detector lost none	< 0.00001
Diffuse reflectance	Top surface is rough. Error found by looking at standard deviation at each angle of 5 runs. The diffuse reflectance is greatest at large angles.	< 0.00001

On the parallel polarisation data (where the signal was small so the noise due to laser instability created a large percentage error), the fitting function was not putting enough weight on the data points at small angles. Therefore I decided to cut out all the data at angles greater than  $65^\circ$ <sup>6</sup>. This made a significant improvement to the fit (from  $n_{fit} = 1.91$  to  $n_{fit} = 1.48$ ) although there was no improvement to the fit on perpendicular polarisation (where reflectance is larger at smaller angles).

#### 4.2.2 Measurements from the bottom

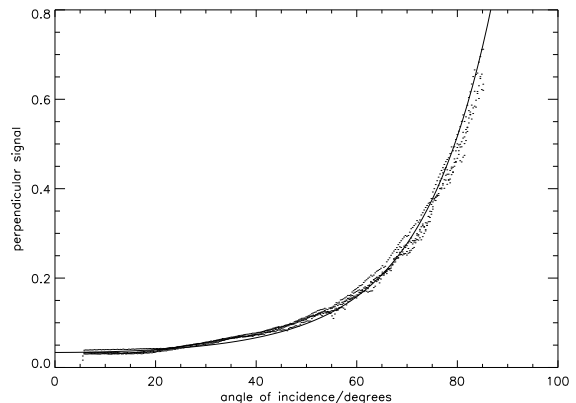
I then tested the instrument by scanning from underneath the glass block, this time expecting to find a refractive index ratio of  $1/1.5 = 0.66$ .

Before taking a measurement, the equipment needed further alignment. In order to position the

<sup>6</sup>this is justifiable as I plotted a graph of parallel reflectance vs incident angle for  $n=1.35$  and  $n=1.45$ , and most of the difference in the two curves lay below an incident angle of  $60^\circ$

Table 2: Results quoted to 3sf

Method	n	standard deviation of n
Fit to perpendicular	1.45	$\pm 0.01$
Fit to parallel for $\theta_i < 65^\circ$	1.48	$\pm 0.01$
Brewster's Angle	$1.38 < n < 1.6$	

Figure 5: A fit of  $n=1.45$  (line) over perpendicular polarisation data (points).

bottom surface normal to the laser, the semicircle needs to be exactly in the centre of the rotation circle.

The maximum possible signal is now lower than for the top measurement, due to absorption within the glass block<sup>7</sup> and reflection from the outside and inside of the curved bottom of the block. Now I could not directly measure the maximum signal. I planned to estimate the maximum signal by measuring the absorption within the glass block and estimating the reflection using the refractive index found by the top surface measurement and equation (11). However, I was unable to measure the absorption as the laser spot was finite sized, so the spot was focussed as it left the block at the curved surface. I ended up estimating the maximum signal

<sup>7</sup>I know my glass absorbs red light as it looks green in daylight

Figure 6: A fit of  $n=1.48$  (line) over parallel polarisation data (points).

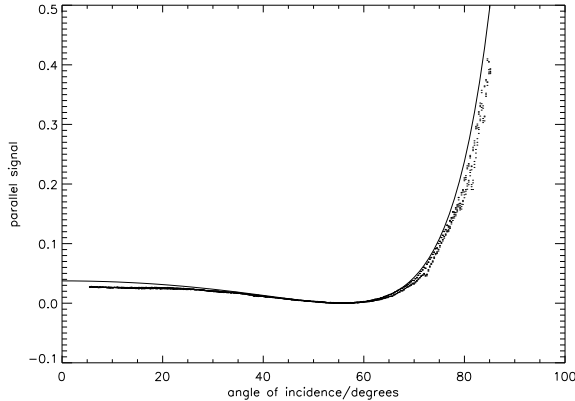
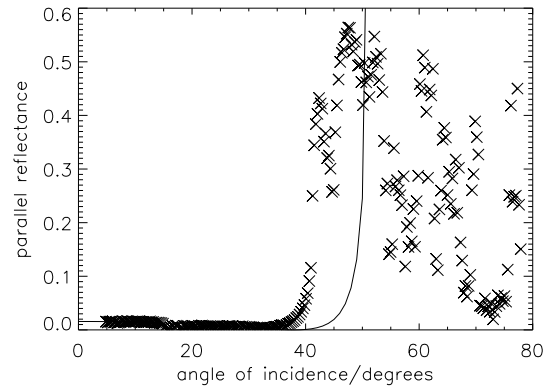


Figure 7: A fit of  $1/n=0.777$  (line) on data of parallel polarisation (crosses), from the bottom.



by measuring the signal with the laser and detector  $180^\circ$  apart, with the glass block in the middle. In fact, during a measurement the beam travels twice as far as this through the material and is defocused as well as focused, giving me an error of up to 20% in laser power and a standard deviation of 0.5 in fitted refractive index. It is clear that a better method of determining total power is necessary.

In the array of errors that I passed to the fitting function, I assumed that the surface roughness of the bottom of the top surface was the same as for the top. As well as diffuse reflectance from the top surface, there was a large systematic error at angles greater than the critical angle from imperfections of the glass interior itself - evident in the large systematic variation in reflectance, see a plot of two scans in the appendix in section F. The probability of losing a step is also larger, now that the laser has to move more steps from the stop. There is an additional systematic error as the bottom of the semicircle is badly machined and not circular, affecting reflectance at all angles of incidence.

The fitting function gave  $1/n = 0.777 \pm 1.4$ , see figure 7 for a graph of the results. This differs markedly from the expected 0.66, although I am not surprised, as the data does not resemble the model.

I wrote a program in IDL to work out the critical angle by finding the angle at which the change in reflectance with angle was greatest. This program worked very well on simulated results with

noise levels comparable to those of measurements on the top surface. However, the real data above the critical angle were so noisy that the largest gradient in the reflectance-angle curve was well above the visible critical angle. So, I decided to try to find the critical angle by eye, using the graph in figure 7. This gave a critical angle between  $41 < \theta_c < 43^\circ$  giving  $0.0656 < 1/n < 0.682$ .

The data given by this equipment is clearly too noisy to be used to work out the refractive index of the aerosol.

#### 4.2.3 The second design

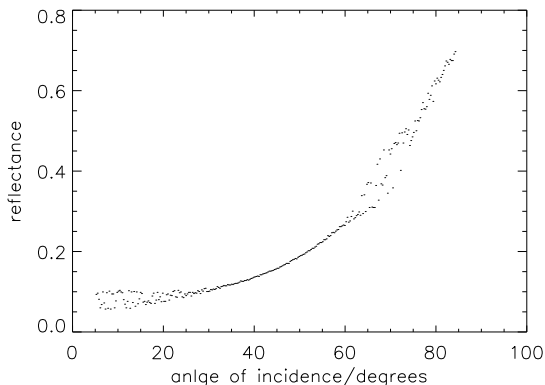
I then decided to try using a thin piece of glass as a sample holder. I rewrote the interpreting program in IDL, so take in to account the reflections from both the bottom and top surface of the glass. However, when the experiment was run, the data was much more complicated than before, see figure 8.

At some angles, I think the secondary or tertiary reflections were interfering with the signal. This technique was not explored further.

#### 4.2.4 The third design

I then considered turning the semicircular glass block on its side, to avoid the poorly machined bottom face and so that the beam was travelling over a smaller path inside the impure glass. I calculated that the reflection from the bottom surface would

Figure 8: Perpendicular reflection from the top of the thin glass slide.



miss the detector; so again, all of the signal would originate from the glass-mixture interface. As the beam is refracted at the bottom interface, I had to make corrections to the software that positions the detector. However, I ran out of time in the laboratory to get any results using this new method.

## 5 Conclusion

I have designed and built a goniometer, which is working, but currently the data is too noisy to get a good measurement of the refractive index of an aerosol.

If it were possible to get a sample holder of much better purity, and whose circular face had been machined to a tolerance similar to that of the surface roughness of the top surface, I think that it would be possible to use the equipment to work out the refractive index of an aerosol. If a sample holder could be sourced such that the error on the data could be reduced to that of the top surface (i.e. mostly from laser instability, giving a standard deviation of 0.04 on the fitted refractive index ratio) and using a mixing fraction of 1.2% aerosol, as in [8], (giving a standard deviation of 0.0066 on the mixing ratio if you make up  $100\mu g$ ); by propagating the errors through the calculation of the aerosol refractive index, using equation (12)

$$n_{\text{aerosol}} = \frac{n_{\text{solution}} - n_{\text{water}} \text{fraction}_{\text{water}}}{\text{fraction}_{\text{aerosol}}} \quad (16)$$

I have calculated that the real refractive index should be able to be found to within a standard deviation of 0.06 using MPFITFUN.

## 6 Further Work

In order to make further progress, a good quality semicircular sample holder has to be purchased or machined. Running MPFITFUN on the data should give the real refractive index to within a standard deviation of 0.06. The limiting factor on the measurement would be the stability of the laser. If this could be reduced to 10% of the current value, either by monitoring the laser power whilst taking a scan via a beam splitter, or by purchasing a more stable laser, I have calculated that the real refractive index could be found to within a standard deviation of 0.01.

In order to find the real and imaginary parts of the refractive index of the aerosol, another (multivariate) least squares fitting function will need to be sourced. Currently MPFITFUN can only find one parameter at a time, so can't fit both the real and imaginary parts of the refractive index.

In the future it would be wise to get a more stable sample holding system, as this one was liable to rocking or being knocked and took a long time to align, and to think of a more secure way of holding the laser, as the laser would tend to shake itself around in the clamp as it knocked against the stop.

### 6.1 Acknowledgements

Thanks to Peters, D.M, Chack, A. Bowles, N. and Thomas, I. of the AOPP department, University of Oxford for their help with this project.

## A Appendix : References

### References

- [1] McConnell, C.L Formenti, P. Highwood, E.J. and Harrison, M.A.J. (2009) Using aircraft measurements to determine the refractive index of Saharan dust during the DODO experiments, *Atmos. Chem. Phys. Discuss.*, 9, 23505-23546,
- [2] Peters, D.M. McPheat, R.A. Grainger, R.G. Thomas, G. Irshad,R. (2010). *Lecture Hand-out Aerosol Spectroscopy, Fire, Earth, Air and Water*. University of Oxford.
- [3] Solomon, S., D. Qin, M. Manning, R.B. Alley, T. Berntsen, N.L. Bindoff, Z. Chen, A. Chidthaisong, J.M. Gregory, G.C. Hegerl, M. Heimann, B. Hewitson, B.J. Hoskins, F. Joos, J. Jouzel, V. Kattsov, U. Lohmann, T. Matsuno, M. Molina, N. Nicholls, J. Overpeck, G. Raga, V. Ramaswamy, J. Ren, M. Rusticucci, R. Somerville, T.F. Stocker, P. Whetton, R.A. Wood and D. Wratt, (2007): Technical Summary. In: *Climate Change 2007: The Physical Science Basis*. In: *Fourth Assessment Report of the Intergovernmental Panel on Climate Change*, Cambridge University Press.
- [4] Highwood, E.J. (2009), Suggested refractive indices and aerosol size parameters for use in radiative effect calculations and satellite retrievals, *ADIANT / APPRAISE CP2 Technical Report, DRAFT V2*.
- [5] Patterson, E. M., Gillette, D. A. and Stockton, B.H. (1977), Complex Index of Refraction Between 300 and 700 nm for Saharan Aerosols, *J. Geophys. Res.*, 82(21), 3153-3160.
- [6] Thomas, G.E , Bass, S.F. Grainger, R.G. and Lambert, A. (2005) spectra with a damped harmonic-oscillator band model, , 1332 *APPLIED OPTICS/ Vol. 44, No. 7*
- [7] Patterson, E.M and Pollard, C.O, (1983) Optical properties of the ash from El Chichon Volcano, *Geophysical Research Letters*, Vol.10, No. 4, 317-320

- [8] Garca-Valenzuela, A. Barrera, R.G. Snchez-Prez, C. Reyes-Coronado, A. and Mndez , E.R. (2005) Coherent reflection of light from a turbid suspension of particles in an internal-reflection configuration: Theory versus experiment., *OPTICS EXPRESS* Vol. 13, No. 18 / 6730
- [9] Zhang, C. Wang Song, Q. Ku, C. Gross, R.B, Birge, R.R (1994) Determination of the refractive index of a bacteriorhodopsin film, *OPTICS LETTERS* Vol. 19, No. 18
- [10] Hapke, B. (1993) ‘Theory of Reflectance and Emittance Spectroscopy`, Cambridge University Press (pg 0 - 455)
- [11] <http://www.arduino.cc/en/Main/ArduinoBoardDuemilanove>
- [12] Markwardt, C. B. (2008), “Non-Linear Least Squares Fitting in IDL with MPFIT,” *Astronomical Data Analysis Software and Systems XVIII*, Vol. 411, p. 251-254

## B Appendix : Fresnel Equations for absorbing medium

The Fresnel equations 17 and 18 for complex an absorbing medium.

$$R_{\parallel} = \frac{[(n^2 - \kappa^2)\cos\theta_i - G_1]^2 + [2n\kappa\cos\theta_i - G_2]^2}{[(n^2 - \kappa^2)\cos\theta_i + G_1]^2 + [2n\kappa\cos\theta_i + G_2]^2}, \quad (17)$$

$$R_{\perp} = \frac{[\cos\theta_i - G_1]^2 + G_2^2}{[\cos\theta_i + G_1]^2 + G_2^2}, \quad (18)$$

where

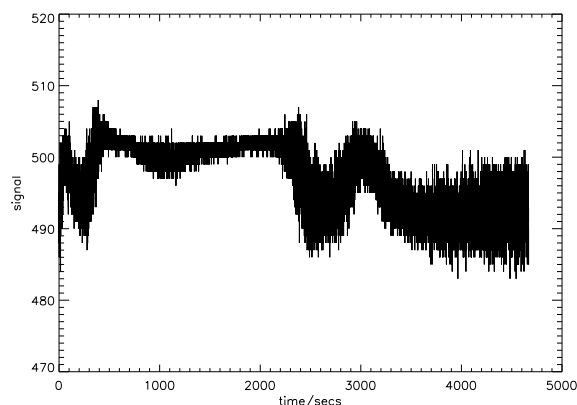
$$G_1^2 = \frac{1}{2}\{[n^2 - \kappa^2 - \sin\theta_i^2] + [(n^2 - \kappa^2 - \sin\theta_i^2)^2 + 4n^2\kappa^2]^{1/2}\}, \quad (19)$$

$$G_2^2 = \frac{1}{2}\{-[n^2 - \kappa^2 - \sin\theta_i^2] + [(n^2 - \kappa^2 - \sin\theta_i^2)^2 + 4n^2\kappa^2]^{1/2}\}. \quad (20)$$

## C Appendix : Laser power

To investigate the stability of the laser I took a measurement of laser power over 1 hour 30 minutes. See figure 9 for the results.

Figure 9: The signal from the detector of the laser power over 1hr 30mins



## D Appendix : Electronics

For a picture of the electronics see figure 10

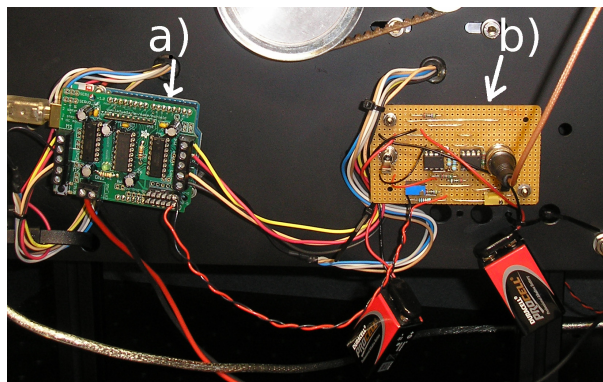


Figure 10: A picture of the electronics. a) Arduino board and motor shield kit. b) Amplifier circuit.

## E Appendix : Aligning

- Move detector  $180^\circ$  from laser. Adjust laser pole length until the spot lands upon detector centre.
- Set polarisation of laser by rotating it within its mount until the maximum power is incident upon the detector with polariser at  $45^\circ$ . Check that the power is similar for parallel and perpendicular polarisations.
- Suspend a cross in front of the laser spot. Move the laser  $180^\circ$ , then rotate laser pole within clamp in rod and adjust screw tightness on pulley face until spot lands upon cross when laser is in both positions.
- Set glass semicircle height by eye, and inclination with inclinometer.
- Move laser to horizontal, adjust position and tilt of glass semicircle until the laser travels through the middle of each edge.
- Move laser to estimated normal, set laser to retro-reflect by adjusting second screw on prism mount.
- Set semicircle height exactly using the translating post holder by making sure laser spot does not move on the surface of the glass slide during a scan.
- Find normal (within half a step) by finding where the specular reflection lands on the detector from various angles of incidence.

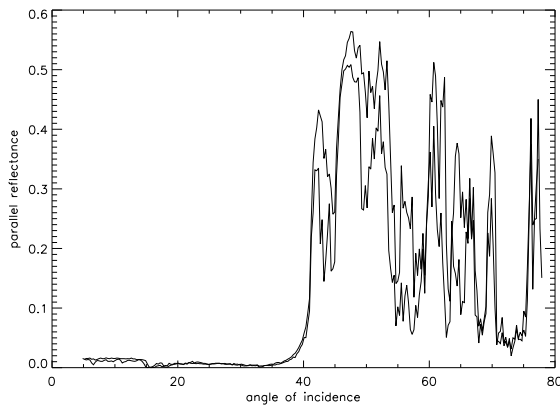
## F Appendix : Two scans from bottom

See figure 11 for a plot of data from two scans from the bottom of the glass block.

## G Appendix : Detector response

The detector is finite sized, so the laser spot does not need to be directly incident upon the middle of the detector face. This means that the equipment

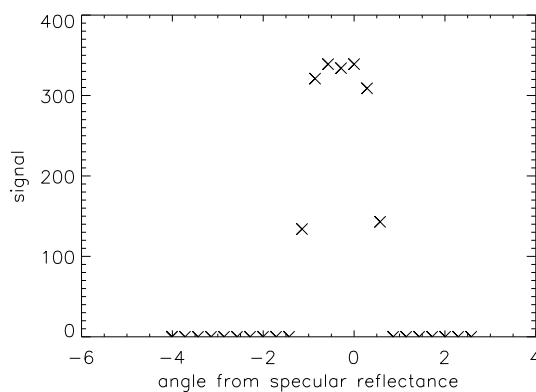
Figure 11: A plot of two scans from the bottom. Note the large systematic error at angles greater than the critical angle. Data plotted as lines to emphasise the systematic error.



has some tolerance for being misaligned. However, the detector response is not uniform over all the face. See figure 12 for a graph of this response function.

See figure 12 for a graph showing the detector response function.

Figure 12: Response of the detector



## H Appendix : Sketches

### H.1 Continuous reading

```
//sketch to take CONTINUOUS READINGS
//FROM ANAGLOG PIN

int val;
int analogPin = 5;

void setup(){
  Serial.begin(2400);
  Serial.println("#rotating laser");
}

void loop(){
  val = analogRead(analogPin);
  Serial.println(val);
  delay(200);
}
```

### H.2 The controlling sketch

```
//sketch to use on experiment
#include <AFMotor.h>

AF_Stepper motorL(200, 1);
//stepper motor on M1 M2 w 200
//steps/revolution
AF_Stepper motorD(200, 2);
//stepper motor on M3 M4 w 200
//steps/rev

// defining all the integars
int x, y, rl, rd, RL, RD, r0, r1, r2, r3,
  r4, r5, r6, r7, r8, r9, Lposition,
  Dposition, i, j, k, l, d, z, reading;
unsigned long N, a, b, c;
char Str[80];
unsigned long A= 1; //number of
//values over which we
//wish to average
int analogPin = 5;

void setup() {
  Serial.begin(2400); //initialise serial
  //communication
  Serial.println("#The program begins!");
  motorL.setSpeed(1);
```

```

//set motor speed 1rpm
motorD.setSpeed(1);
//set motor speed 1rpm

//in case you set it to home before
//starting the program
Lposition=0;
Dposition=0;
}

void loop() {
getSerial(); //read in command
// string from serial port

// if you want to scan
if(Str[0] == 'S')
{if( Str[1] == 32 && Str[6] == 32
&& Str[11] == 32 && Str[16] == 32
&& Str[21] == 32 && Str[24] == 32)
//make sure it is in correct format
{
//positioning laser
i=1000*(Str[2] - 48); //second
//digit of string indicates
position of 100s of steps for laser
j=100*(Str[3] - 48); // 3rd digit
//of string is position of 10s of
//steps for detector
k=10*(Str[4] - 48);
l=Str[5] - 48;
rl=i+j+k+l - Lposition; //get the right
// number of laser steps from current
// position
Lposition=i+j+k+l; // save current
// position
if(rl>0)
{ motorL.step(rl, BACKWARD,
INTERLEAVE); } // move laser
// clockwise if new position is further
//from home than the old
if(rl<0)
{ rl=-rl;
motorL.step(rl, FORWARD,
INTERLEAVE); } // move laser
// anticlockwise if new position is
//closer to home than the old

//positioning detector
i=1000*(Str[7] - 48); //5th digit of
//string indicates position
//of 100s of steps for laser
j=100*(Str[8] - 48); // 6th digit of
//is position of 10s of steps for
//detector
k=10*(Str[9] - 48);
l= Str[10] - 48;
rd=i+j+k+l-Dposition; // get the right
// number of laser steps from current
//position
Dposition=i+j+k+l; // save current
//position
if(rd>0)
{motorD.step(rd, BACKWARD,
INTERLEAVE); } //move laser
//clockwise if new position is further
// from home than the old
if(rd<0)
{rd=-rd;
motorD.step(rd, FORWARD,
INTERLEAVE); } // move laser
//anticlockwise if new position is
// nearer to home than the old

//work out final position of laser
i=1000*(Str[12] - 48); //second
//digit of string indicates
//final position of 100s of steps for
//laser
j=100*(Str[13] - 48); // 3rd digit
//of string is position
//of 10s of steps for detector
k=10*(Str[14] - 48);
l=Str[15] - 48;
rl=i+j+k+l - Lposition; //get the
// distance of final position from
//current position
RL=10*(Str[22]-48) + (Str[23]-48);
// read in laser resolution

//work out final detector position
i=1000*(Str[17] - 48);
j=100*(Str[18] - 48);
k=10*(Str[19] - 48);
l=Str[20] -48;
rd=i+j+k+l - Dposition;
RD=(10*(Str[25] - 48) + Str[26] -48);
N=0;
READING(); // take first reading at

```

```

//first
if(rl>=0 && rd>=0) // if the final
//positions are further from home,
// move clockwise
{ // r/R = number of steps
  for(N==0; N<r1/RL; N++)
  {motorL.step(RL, BACKWARD,
  INTERLEAVE);
  Lposition = Lposition+RL;
  motorD.step(RD, BACKWARD,
  INTERLEAVE);
  Dposition = Dposition + RD;
  READING();}
}

if(rl>=0 && rd<0)
{ // r/R = number of steps
  for(N==0; N<r1/RL; N++)
  { motorL.step(RL, BACKWARD,
  INTERLEAVE);
  //move clockwise
  Lposition = Lposition+RL;
  motorD.step(RD, FORWARD,
  INTERLEAVE);
  //move anticlockwise
  Dposition = Dposition - RD;
  READING();}
}

if(rl<0 && rd>=0)
{ rl=-rl;
// r/R = number of steps
for(N==0; N<r1/RL; N++)
{ motorL.step(RL, FORWARD,
  INTERLEAVE); //move
//anticlockwise
Lposition = Lposition-RL;
motorD.step(RD, BACKWARD,
  INTERLEAVE); //move clockwise
Dposition = Dposition + RD;
READING();}
}

if(rl<0 && rd<0)
{ rl=-rl;
// r/R = number of steps
for(N==0; N<r1/RL; N++)
{ motorL.step(RL, FORWARD,
  INTERLEAVE); //move
//anticlockwise
Lposition = Lposition-RL;
motorD.step(RD, FORWARD,
  INTERLEAVE); //move
}

//anticlockwise
Dposition = Dposition - RD;
READING();}
}

//to scan just the detector
if(Str[0] == 'D') //you want to keep
//the laser still and scan the detector
{ if(Str[1]== 32 && Str[6]==32
&& Str[11]==32) //check format
{ //positioning laser
i = 1000*(Str[2] -48); //second
//digit of string indicates position of
//100s of steps for laser
j= 100*(Str[3] -48); // 3rd digit of
// string is position of 10s of steps
// for detector
k=10*(Str[4] - 48);
l = Str[5] -48;
rl = i + j+ k+l - Lposition; //get
//the right number of laser steps
//from current position
Lposition = i+j+k+l; // save
//current position
if(rl>0)
{motorL.step(rl, BACKWARD,
  INTERLEAVE);}
// move laser clockwise if new
//position is furtherfrom home
//than the old
if(rl<0)
{ rl=-rl;
motorL.step(rl, FORWARD,
  INTERLEAVE);}
//move laser anticlockwise if new
//postion is closer to home than the
//old

//positioning detector
i = 1000*(Str[7] -48); //5th digit of
//string indicates positionof 100s of
// steps for laser
j= 100*(Str[8] -48); // 6th digit of
// string is position of 10s of steps
// for detector

```

```

k= 10* (Str[9] - 48);
l= Str[10] - 48;
rd = i + j+ k +1 - Dposition; // get
//the right number of laser steps
//from current position
Dposition = i+j+k+1; // save
//current position
if(rd>0)
{motorD.step(rd, BACKWARD,
INTERLEAVE);}
// move laser clockwise if new
//position is further from home than
// the old
if(rd<0)
{ rd=-rd;
  motorD.step(rd, FORWARD,
INTERLEAVE);}
//move laser anticlockwise if new
// position is
//nearer to home than the old
}

//work out final detector position
i=1000*(Str[12] -48);
j=100*(Str[13] -48);
k=10*(Str[14] - 48);
l=Str[15] -48;
rd=i+j+k+1 - Dposition; //rd is no of
//steps you have to move during the
//scan
READING(); // take first reading
//at first
N=0;
if(rd<0)
{for(N==0; N>rd; N--)
{motorD.step(1, FORWARD,
INTERLEAVE);}
//step once anticlockwise
READING();
Dposition=Dposition-1;}
}
if(rd>0)
{for(N==0; N<rd; N++)
{motorD.step(1, BACKWARD,
INTERLEAVE);}
READING();
Dposition=Dposition+1;}
}
}
else{ Serial.println('# Error in
command');} //the format is wrong
}

//you want to go to the home position
if(Str[0] == 'H')
{motorD.step(640, FORWARD,
SINGLE);}
//move both detectors anticlockwise
// til they hit the stop
motorL.step(640, FORWARD,
SINGLE);
Lposition=0;
Dposition = 0; }

//you want to nudge in to home
//position
if(Str[0] == 'N')
{if(Str[2] == 'D' && Str[3] == 'C')
{motorD.step(1, BACKWARD,
INTERLEAVE);
Lposition=0;
Dposition = 0;}}
if(Str[2] == 'D' && Str[3] == 'A')
{motorD.step(1, FORWARD,
INTERLEAVE);
Lposition=0;
Dposition = 0;}}
if(Str[2] == 'L' && Str[3] == 'C')
{motorL.step(1, BACKWARD,
INTERLEAVE);
Lposition=0;
Dposition = 0;}}
if(Str[2] == 'L' && Str[3] == 'A')
{motorL.step(1, FORWARD,
INTERLEAVE);
Lposition=0;
Dposition = 0;}}
}

//you want to move and read
if(Str[0] == 'M')
{if(Str[1] ==32 && Str[6] ==32)
//if there are spaces in the right place
{ //positioning laser
i= 1000*(Str[2] -48); //second digit
// of string indicates position of
//1000s of steps for laser
j= 100*(Str[3] -48); // 3rd digit
//of string is position of 100s of
//steps for detector

```

```

k= 10*(Str[4] - 48); //
l= (Str[5] -48);
rl= i + j+ k +l - Lposition; //get the
// right number of laser steps from
// current position
Lposition = i+j+k+l; // save current position
if(rl>0)
{ motorL.step(rl, BACKWARD,
INTERLEAVE);}
//move laser clockwise if new position
//is further from home than the old
if(rl<0)
{ rl=-rl;
motorL.step(rl, FORWARD,
INTERLEAVE); }
//move laser anticlockwise if new
//position is closer to home than the
//old

//positioning detector
i = 1000*(Str[7] -48); //second digit
//of string indicates position of 1000s
//of steps for laser
j= 100*(Str[8] -48); // 3rd digit of
//string is position of 100s of steps
//for detector
k=10*(Str[9] - 48); //
l = (Str[10] -48);
rd = i + j+ k +l - Dposition;
// get the right number of laser
//from current position
position = i+j+k+l; // save current
//position
if(rd>0)
{motorD.step(rd, BACKWARD,
INTERLEAVE);}
//move detector clockwise if new
//position is further from home
//than the old
if(rd<0)
{rd=-rd;
motorD.step(rd, FORWARD,
INTERLEAVE);}
//move detector anticlockwise if
//new position is nearer to home
//than the old
READING();//after you have
//positioned the laser and detector,
//take a reading
}

else{Serial.println("# Error in
command"); }
}

// if you want to take a reading
if(Str[0] == 'R')
{ READING(); }

//You have called the help function
if (Str[0] == '??')
{
Serial.println("#");
Serial.println("#");
Serial.println("# '?' Calls Help
function");
Serial.println("#");
Serial.println("# 'H' Sends arms to
the stop and sets that as
000 000");
Serial.println("#");
Serial.println("# 'N' Calls nudge
function and sets position
to 000 000");
Serial.println(" N LC laser one
clockwise, N DA detector
one anticlockwise");
Serial.println("#");
Serial.println("# 'R' Takes a reading
from the detector");
Serial.println("#");
Serial.println("# 'M' Calls Move function,
Input M 000 000");
Serial.println("# M L D where
L=laser, D=detector");
Serial.println("#");
Serial.println("# 'S' Calls Scan
function as
S 0000 0000 0000 0000 00 00");
Serial.println("# S Li Di Lf Df Lr Dr,
where i=initial, f=final,
r=resolution");
Serial.println("#");
Serial.print("# Laser position ");
Serial.println(Lposition);
Serial.print("# Detector position ");
Serial.println(Dposition);
reading = analogRead(analogPin);
Serial.print("# Detector reading ");
}

```



```
Serial.print(" ");  
Serial.print(r3);  
Serial.print(" ");  
Serial.print(r4);  
Serial.print(" ");  
Serial.print(r5);  
Serial.print(" ");  
Serial.print(r6);  
Serial.print(" ");  
Serial.print(r7);  
Serial.print(" ");  
Serial.print(r8);  
Serial.print(" ");  
Serial.println(r9);  
}
```